Semiconductor Physics, Quantum Electronics & Optoelectronics, 2024. V. 27, No 2. P. 235-241.

Optoelectronics and optoelectronic devices

Spectral features of pristine and irradiated white emitting InGaN LEDs with quantum wells

O.P. Budnyk[1], M.E. Chumak[2], D.P. Stratilat[3], V.P. Tartachnyk[3]

[1]*Institute of Physics, National Academy of Sciences of Ukraine*
[2]*Ukrainian State Mykhailo Drahomanov University, Kyiv, Ukraine*
[3]*Institute for Nuclear Research, National Academy of Sciences of Ukraine*
[*]*Corresponding author e-mail: oksana.budnyk@gmail.com*

Abstract. The emission spectra of InGaN/GaN white light emitting diodes (WLEDs) were measured. The main emission components were a LED blue line with λ_{max} = 443 nm and a wide double band in the range of 500…650 nm of the secondary emission of AIT-YAG phosphor (Ce). The observed non-monotonic temperature dependence of the emission was attributed to the electric-field screening effect by mobile carriers as well as to thermal quenching due to the increased density of the phonon gas. The power conversion factor of phosphor emission increased in the temperature range of 200…290 K. The total energy losses for the Stokes shift were 82% and 77% for the first (blue) and the second band, respectively. The decrement of emission at high injection currents (over 20 mA) was attributed to ballistic transfer of carriers above the quantum wells and subsequent non-radiative recombination in the barrier layers. The existence of long-term relaxation processes in the white LEDs was assumed to be due to the accumulation of In atoms. Electron beam irradiation caused WLED efficiency degradation due to the introduction of deep traps in the quantum well region. The radiation resistance of the AIT-YAG phosphor was ~1.6 times higher than that of the InGaN part.

Keyworlds: white LEDs, InGaN, AIT-YAG, gamma-irradiation, spectral characteristics of white LEDs.

https://doi.org/10.15407/spqeo27.02.235
PACS 42.88.+h, 85.60.Jb

Manuscript received 03.05.24; revised version received 27.05.24; accepted for publication 19.06.24; published online 21.06.24.

1. Introduction

Gallium nitride is a direct band gap ($E_g^{300K} = 3.44\,\text{eV}$) $A^{III}B^{V}$ semiconductor, which crystallizes either in hexagonal phase (α-phase, thermodynamically stable, wurtzite) or cubic phase (β-phase, metastable, zinc blende). The structures of these phases differ in the packing sequence of nitrogen and gallium rows. In the preffered wurtzite GaN, nitrogen anions and gallium cations alternate along the polar *c*-axis ⟨0001⟩, leading to a spontaneous polarization and a piezo effect [1–3]. GaN films are grown on sapphire (Al_2O_3) substrates for LED application. The lattice mismatch between the film and the substrate develops if cheaper Si substrates are used. There is also a mismatch between the InN and GaN sublattices in an InGaN solid solution due to a significant difference in the cation radii (R_{Ga} = 0.47 Å, R_{In} = 0.7 Å). Such mismatch reaches 15% in the *c*-direction and affects the dislocation density [1]. A buffer layer allows suppressing propagation of dislocations from the substrate to the active layer.

Three color sources (RGB) emitting at different wavelengths are joined in a LED to produce a high-quality white light. Alternatively, a blue LED source is combined with color converters like cerium-doped aluminum yttrium garnets (Ce:YAG) [4]. LEDs of this type have significant losses due to reradiation (over 20%) and a shorter lifetime compared to RGB LEDs. Moreover, their phosphor often exhibits a long afterglow. Instead, white RGB LEDs are expensive and require an optical system for color emitters and a heat dissipation schema [5]. A balance of colors from different sources in WLED should be maintained to obtain the natural white. The current power supply modes (continuous and pulsed) affect the colorimetric parameters (such as chromaticity coordinates, correlated color temperature and color rendering index) due to different impact on the color sources (internal factor). Irradiation with accelerated particles (external factor) has a similar impact. Both factors perturb the color balance of WLEDs. To maintain it, temperature-current dependence of the spectral characteristics as well as the information

on the underlying mechanisms are needed. Studies on radiation degradation of optoelectronic devices allow determining the radiation constants of the constituting materials and developing the ways to use penetrating radiation to adjust the device parameters, including the emission profile, in a desired manner.

Recently, highly efficient monolithic WLEDs and WLED with quantum wells (QWs) have been obtained. For instance, an electrically controlled phosphor-free monolithic WLED consists of a blue-emitting (λ_1 = 427 nm) QW upper layer and a yellow-emitting (λ_2 = 560 nm) QW lower layer [6]. The dimensions of these micro-LEDs of 40×40 μm and 20×20 μm allow overcoming the high-frequency pulse excitation restrictions. There are high-quality quantum dot LED displays, matching three emission lines of 630, 520, and 450 nm as RGB [7, 8]. A monolithic InGaN WLED with λ_1 = 445 nm and λ_2 = 560 nm and the diode size range of 20 to 40 μm was produced on sapphire [9]. This diode is capable of transmitting ≈ 3 dB, 660 MHz and may be utilized for backlighting in liquid crystal displays. Non-radiative energy transfer between the objects, separated by the distance 10 times larger than their size (Förster resonance energy transfer), has been observed in monolithic LED structures [10, 11].

Influence of penetrating radiation on InGaN/GaN WLEDs grown from InGaN solid solution has been reported in a modest number of works [5, 12–15]. The main outcomes include observation of improved radiation resistance of the studied LEDs [5] and the 'red' and 'blue' spectral shifts after irradiation [12]. Despite some technological challenges like matching the lattice parameters of the InGaN/GaN layers and processing semiconductors under high temperature and high pressure conditions, the field of materials for optoelectronics expands further. Therefore, the demand for new products remains high [16]. WLEDs may improve workplace illumination quality being integrated into the light sources with adjusted spectral emission [17]. Combined with other LEDs, they find their place in greenhouse illuminating systems favoring plant growth and productivity [18]. Furthermore, long-lasting relaxation of spectrally excited semiconductors remains understudied. Such relaxation is accompanied by signal distorsions and slowing of optrons. This work addresses the issues of detection and interpretation of the relaxation process in InGaN/GaN WLEDs.

2. Experimental

We studied hybrid type white LEDs, the active element of which was a blue InGaN/GaN LED with λ_{max} = 443 nm. The wavelength converter was a cerium-doped AIT-YAG ($Y_3Al_5O_{12}$) phosphor with a wide luminescence band in the range of 500 to 650 nm.

Before irradiation, the epoxy lens was polished in order to reduce the energy loss of the electron beam and the effect of lens darkening on the LED radiation intensity.

Irradiation with electrons with E = 2 MeV took place in a pulse mode on a Linear Pulse Accelerator (ILU-6) at a beam current I = 4 mA. The temperature during irradiation was maintained close to 300 K by intensive air cooling. The density of the electron flow varied from 10^{14} to 10^{16} cm^{-2}.

The spectra of the original and irradiated LEDs were measured in the temperature range of 77 to 290 K using an automatic green-wave spectrometer produced by the StellarNet company.

3. Results

The primary radiation source for the white LEDs studied in this work was a blue $In_xGa_{1-x}N$/GaN LED with λ = 443 nm. The yellow phosphor YAG (Cr) acted as an additional emitter, which provided a natural-like emission.

The direct band gap of InGaN solutions allows fabricating highly efficient LEDs in the visible and near UV ranges. Among them, blue-emitting LEDs are distinguished by the highest quantum yield (η ≈ 80%). A moderate concentration of In (x = 0.23%) makes it possible to partially avoid the negative impact of non-radiative levels associated with indium clusters and to reduce the influence of mismatch dislocations between the InGaN and GaN layers.

Aluminum yttrium garnet is a sensitizer-doped Ce^{3+}-crystal with the lattice parameter of 12.01 Å, the band gap E_g = 6.43 eV, and the melting temperature T_{mel} = 1970 °C. Ce ions in a 3+ or 4+ charge state can be localized in the Y_2O_3 sublattice, substituting yttrium ions. Ce^{3+} ions are optically active. In the YAG excitation spectrum, the band at 400…500 nm is the most active. Therefore, combination of LEDs emitting in the range of 400 to 480 nm with a YAG (Ce^{3+}) creates conditions for obtaining a white source [17].

Figs. 1a and 1b show the spectra of a white diode recorded at the temperatures of 77 to 290 K (Fig. 1a) and at different current values (Fig. 1b). The radiation of the InGaN QW (Fig. 1b) presents a narrow Gaussian profile (Fig. 2) with a half-width Δλ = 8 nm and a maximum position at λ_{max} = 443 nm. The spectrum of the phosphor results from superposition of two broad bands peaked at λ_{max} = 540 nm and λ_{max} = 570 nm, and the first has a band near λ = 525 nm; on the second – near λ = 600 nm. The shapes of these bands are also Gaussian. At this, the half-width of the second Gaussian is difficult to determine since its left half partially overlaps with the first band (Fig. 2).

Temperature dependence of the light intensity of the excitation source is typical for InGaN/GaN LEDs and has a broad maximum, after which close to linear quenching is observed (Fig. 3).

The growth of I_{int} (T) is the result of the decrease in the influence of intra-crystalline fields along the c-direction of InGaN with the increase in the shielding effect of released carriers. The thermal quenching is caused by the increase in the number of phonons.

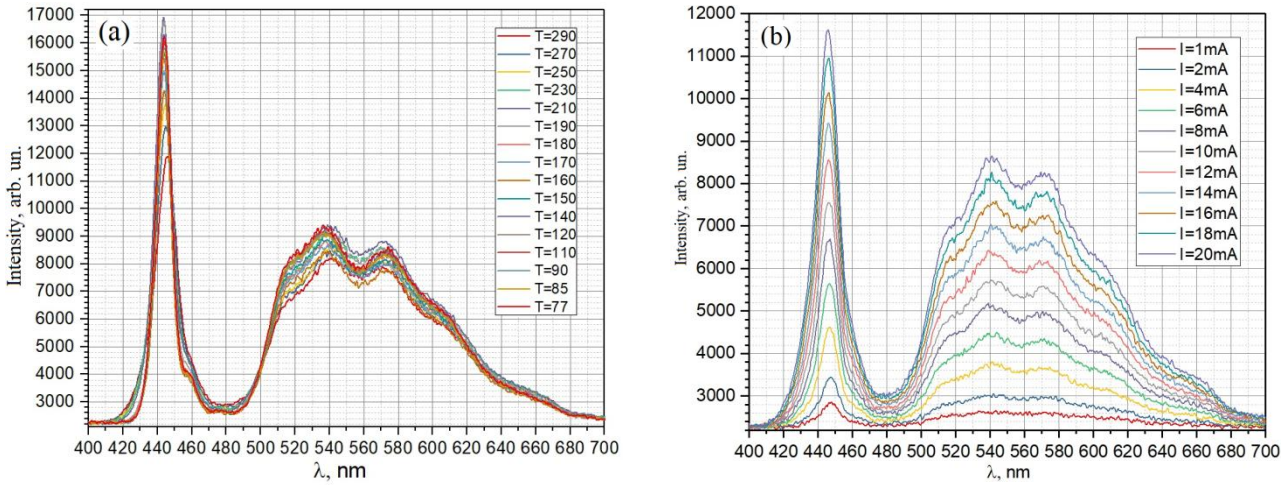

Fig. 1. Spectra of white LEDs measured at different temperatures (a) and different currents at 300 K (b).

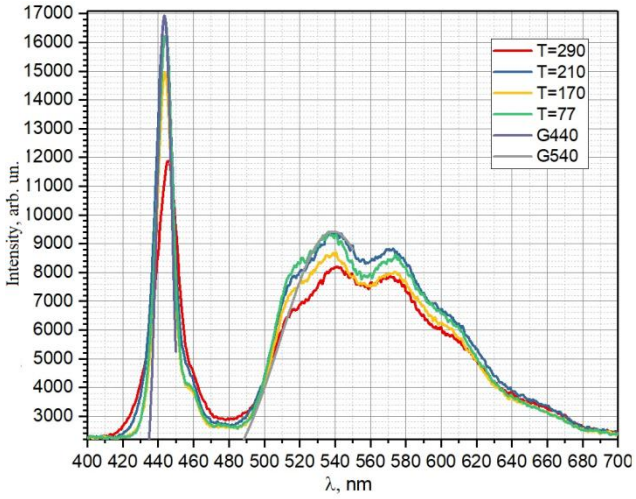

Fig. 2. White LED spectra measured at different temperatures and the Gaussian distributions plotted for the bands peaked at λ_{max} = 443 nm and λ_{max} = 540 nm measured at 77 K.

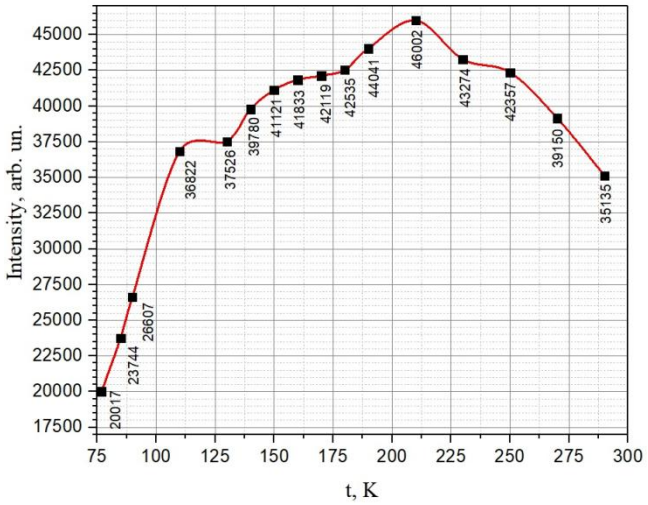

Fig. 3. Temperature dependence of the radiation intensity of the excitation source.

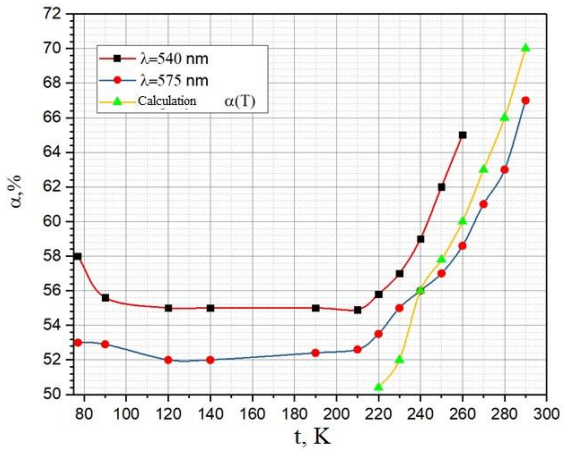

Fig. 4. Temperature dependence of the light power conversion factor of a white LED.

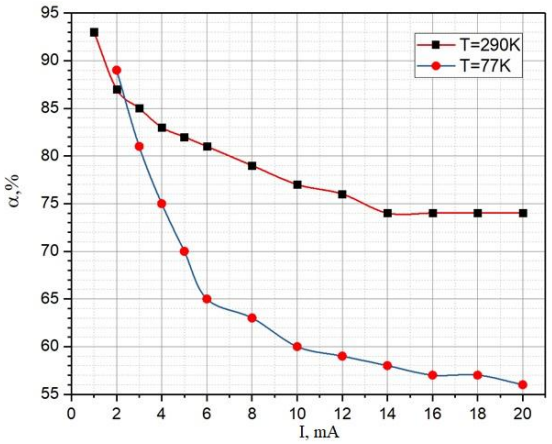

Fig. 5. Dependence of the light power conversion factor on the injection current.

The radiation intensity of the phosphor changes with temperature following the change in the intensity of the excitation source.

The coefficient of conversion of light power by phosphor, which is equal to the ratio of the luminous intensity of the phosphor to the luminous intensity of the LED, $\alpha = \frac{L_{lum}}{L_{\text{LED}}}$, remains almost constant up to 200 K (Fig. 4) and increases at $T > 210$ K due to the sharp drop in L_{LED} as compared to L_{lum}. It is larger at 290 K than at 77 K and slowly decreases at increasing the injection level (Fig. 5). $\alpha(T)$ was calculated using linear temperature dependences of the intensity of LED radiation and the intensity of the phosphor band at $\lambda = 540$ nm in the temperature range of 200…290 K. The results of the calculations also confirmed the growth of the power conversion coefficient in the mentioned temperature range (Fig. 4).

The losses due to the radiation wavelength conversion by the phosphor are $\Delta E_1 = 82\%$ and $\Delta E_2 = 77\%$ for the temperature of 290 K.

Linear growth of each of the three bands is observed in the operating current range (1…20 mA) (Fig. 6). Hence, the integral radiation of the diode also increases at this (Fig. 7). The intensity of this radiation is well approximated by the expression $I_{int} = 0.58\,I$ mA. At $I > 20$ mA, the linear dependence turns into a parabolic one, $y^2 = 2px + c$, where $p = 1.38 \cdot 10^{-5}$ and $c = 0.42 \cdot 10^{-6}$. Slowing down of the growth of the radiation intensity is primarily defined by the decrease in the efficiency of the excitation source at high currents ($I > 20$ mA).

The main reason for the decrease in the number of recombination events in the LED with QW is the specific nanoscale effect of the ballistic transfer of current carriers above crowded wells and their outflow, which is accompanied by their subsequent capture to non-radiative levels localized within the barrier layers.

Existence of such a mechanism of influence on the intensity of radiative recombination in the studied samples can be confirmed by a rapid drop in the quantum yield of the samples with increase in the level of injection (Fig. 8).

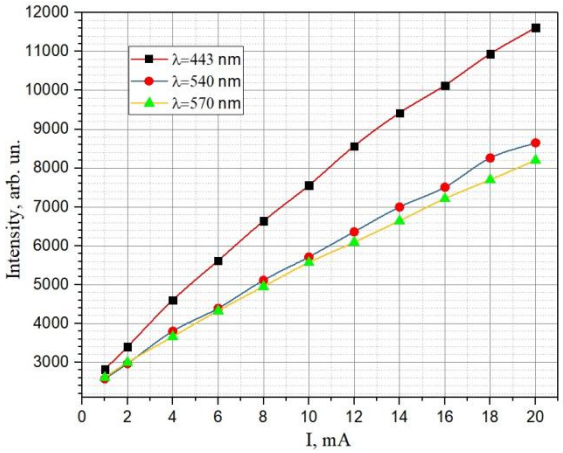

Fig. 6. Dependence of the emission intensity on the current for three radiation bands at room temperature.

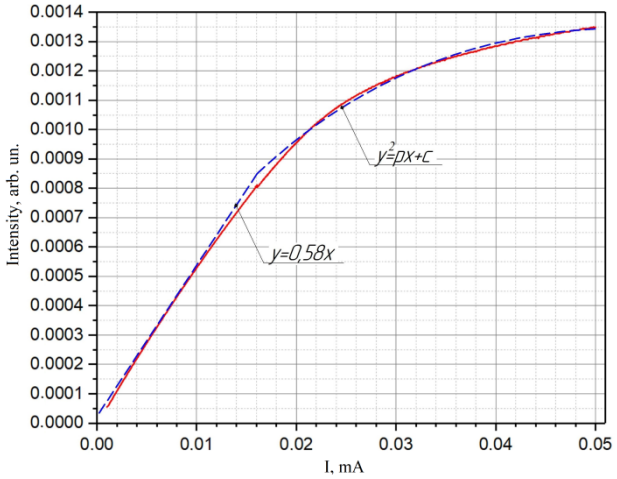

Fig. 7. Dependence of the integrated intensity of LED glow on the current ($T = 300$ K).

QW LED is a complex system that includes a significant number of interfaces between various ultrathin layers with a high density of defects, mainly mismatch dislocations ($\rho_d \approx 10^{10}$ cm^{-2}). All of them lead to appearance of tails of the density of states, which, deforming the zone edges, create conditions for protracted relaxation processes with the duration up to tens of minutes. Similar instability of the electrophysical parameters was previously observed in GaP and InP single crystals, not studied as a part of LEDs.

Taking into account the possibility of using the latter in high-frequency information and computing channels, one should emphasize the importance of detecting and studying relaxation of emissivity, which is the main LED characteristic.

Fig. 9 shows the spectra of the InGaN/GaN LEDs measured after electron irradiation with $F = 1.12 \cdot 10^{15}$ cm^{-2} and during four consecutive time intervals. It can be seen from this figure that after

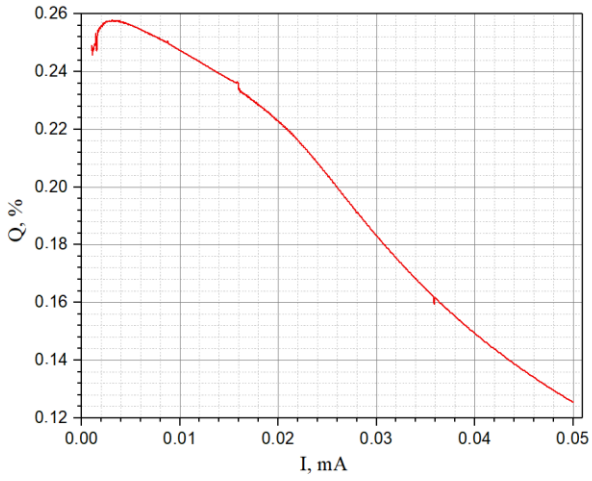

Fig. 8. Dependence of the quantum yield of white LEDs on the diode current ($T = 300$ K).

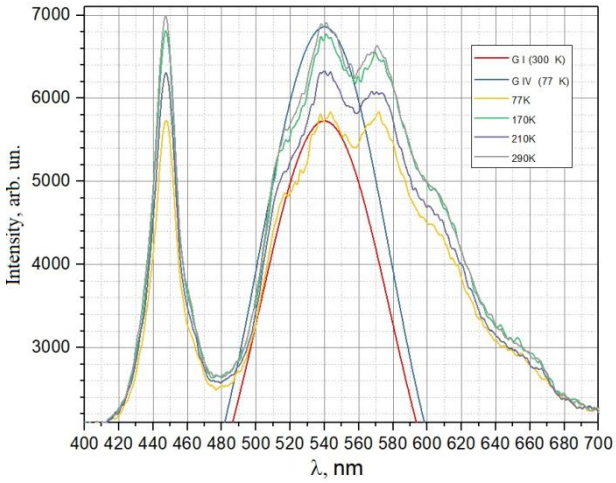

Fig. 9. Spectral distribution of the emission intensity of a white diode. Gaussian distributions for T = 77…290 K are shown.

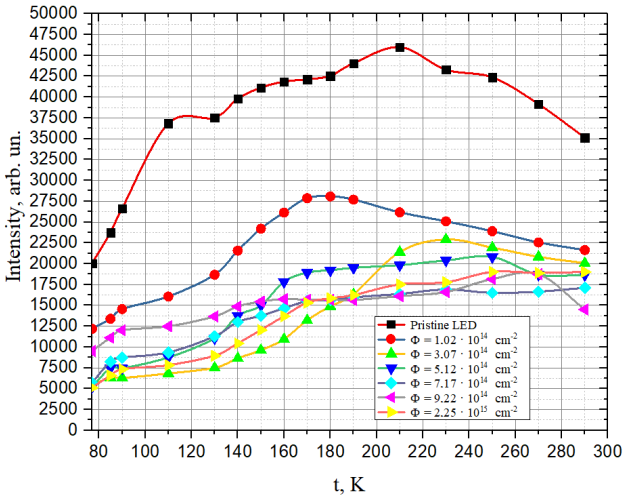

Fig. 11. Temperature dependences of the glow intensity of a white LED measured after different doses of electron irradiation (E_{el} = 2 MeV).

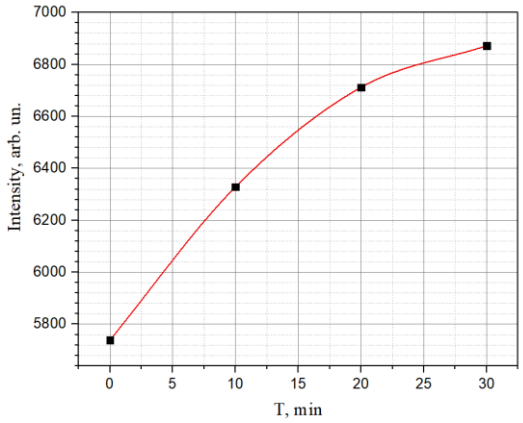

Fig. 10. Change in the integrated intensity of glow after irradiation.

radiation excitation, the intensities of both the main LED line and the two phosphor lines gradually increase and become unchanged after the fourth measurement. During each of the relaxation periods, no additional structure appears on the spectral curves, which indicates configurational stability of the radiative recombination centers. The relaxation changes are caused only by carrier capture and release by the large-scale potential wells levels created by defect clusters, as in GaP and InP homojunctions. In InGaN, such levels can arise within QWs due to clustering of In atoms, which directly follows from the data presented in [17].

Immutability of the relaxation mechanism at all its stages is also evidenced by the same profile of the statistical distribution, namely the normal Gaussian distribution (Fig. 9).

Electron irradiation of white InGaN/GaN LEDs (F = 2.25·10^{15} cm^{-2}) leads to a decrease in the intensity of the recombination glow as a result of the introduction of deep non-radiative levels of radiation defects into the LED active region. A drop in the excitation level is accompanied by a decrease in the brightness of the phosphor glow. If the intensity of LED radiation is halved, the glow of the phosphor decreases by only 1.26 times. Therefore, the radiation resistance of the phosphor turns out to be almost 1.6 times higher than the resistance of LED.

Fig. 10 shows the temperature dependence of the luminescence intensity of the initial and irradiated with different doses blue LED with λ_{max} = 470 nm, which is close to λ_{max} = 450 nm of the excitation source of the white LEDs we studied.

As mentioned above, the shape of the curve $I_{int}(T)$ for the pristine sample reflects the superimposure of two processes, namely shielding of the internal fields of the crystal by free carriers and growth of the phonon density at higher temperatures, which leads to the formation of a broad maximum for the pristine sample. But even a minimal dose of electron irradiation (F = 3.07·10^{14} cm^{-2}) partially smooths the curve and substantially reduces the radiation intensity in the temperature range of 77 to 290 K. The next dose (F =3.07·10^{14} cm^{-2}) reduces the effectiveness of internal field shielding (up to T = 290 K) and has less effect on the phonon scattering of quanta, which prevails at T > 290 K. The following doses (F > 5.13·10^{14} cm^{-2}) lead to equalization of the dependences of $I_{int}(T)$. At this, the temperature boundary between the regions where radiation is affected by the shielding effect of internal fields and the scattering of light by phonons expands and disappears.

It may be noted in conclusion that introduction of radiation defects into the InGaN LED active region induces capture of carriers on the defect deep levels, which participated in shielding of internal piezo fields. Strengthening of the Stark effect causes a decrease in the integral of the overlap of the electron and hole wave functions, and, hence, a decrease in the recombination probability.

4. Conclusions

It was found that the QW emission spectrum of an InGaN/GaN LED, being an active element of the hybrid white LED, is described by a classical Gaussian distribution with a half-width $\Delta\lambda$ = 8 nm and a maximum at λ_{max} = 443 nm. The phosphor radiation consists of two closely spaced lines at λ_{max} = 540 nm and λ_{max} = 570 nm. The temperature dependence of the luminescence intensity of the InGaN LEDs evidences two mechanisms of influence on radiative recombination in the active layer, namely, shielding of internal fields by free carriers at T = 80…120 K and thermal quenching of the luminescence intensity at T > 220 K due to the increase in phonon concentration.

The losses due to the Stokes shift of the phosphor emission at 290 K are ΔE_1 = 82% and ΔE_2 = 77% for the first and the second band, respectively.

Slowing down of the increase of radiation intensity at high currents may be caused by the effect of ballistic transfer of current carriers.

Long-term relaxation processes, which are a consequence of the increased amplitude of the density of states in the sample, are caused by clusters of In atoms.

Electron irradiation of white LEDs introduces radiation defects creating deep levels. Current carriers are captured on these levels, which weakens the shielding of internal fields. Increasing influence of the Stark effect, which reduces the integral of the overlap of the electron and hole wave functions, leads to a drop in the intensity of diode glow.

The radiation resistance of the phosphor turns out to be slightly higher than the resistance of the InGaN LED (by almost 1.6 times) possibly due to the existence of an exciton component in the LED integrated glow.

References

1. Ambacher O. Growth and applications of Group III–nitrides. *J. Phys. D: Appl. Phys*. 1998. **31**. P. 2653. https://doi.org/10.1088/0022-3727/31/20/001.
2. Yu E.T., Dang X.Z., Asbesk P.M. *et al*. Spontaneous and piezoelectric polarization effects in III–V nitride heterostructures. *J. Vac. Sci. Technol. B.* 1999. **17**. P. 1742–1749. https://doi.org/10.1116/1.590818.
3. Ambacher O., Dimitrov R., Stutzmann M. *et al*. Role of spontaneous and piezoelectric polarization induced effects in group-III nitride based heterostructures and devices. *phys. status solidi (b)*. 1999. **216**. P. 381–389. https://doi.org/10.1002/(SICI)1521-3951(199911)216:1<381::AID-PSSB381>3.0.CO;2-O.
4. Schubert E.F. LED basics: Optical properties. In: *Light-Emitting Diodes*. Cambridge University Press. 2006. P. 86–100. https://doi.org/10.1017/CBO9780511790546.
5. Allanche T. *Effect of high radiation doses (MGy) on light Emitting Diodes and optical glasses*. Doctoral thesis from the University of Lyon, 2020. https://theses.hal.science/tel-03215958.
6. Li H., Li P., Zhang H. *et al.* Electrically driven, polarized, phosphor-free white semipolar InGaN light-emitting diodes grown on semipolar bulk GaN substrate. *Opt. Express*. 2020. **28**, No 9. P. 13569–13575. https://doi.org/10.1364/OE.384139.
7. Wu T., Sher Ch.-W., Lin Y. *et al*. Mini-LED and micro-LED: Promising candidates for the next generation display. *Technol. Appl. Sci.* 2018. **8**. P. 1557. https://doi.org/10.3390/app8091557.
8. Chen S.-W.H., Huang Yu.M., Singh K.J. *et al*. Full-color micro-LED display with high color stability using semipolar (20-21) InGaN LEDs and quantum-dot photoresist. *Photon. Res*. 2020. **8**, Issue 5. P. 630–636. https://doi.org/10.1364/PRJ.388958.
9. Khoury M., Li H., Li P. *et al*. Polarized monolithic white semipolar (20–21) InGaN light-emitting diodes grown on high quality (20–21) GaN/sapphire templates and its application to visible light communication. *Nano Energy*. 2020. **67**. P. 104236. https://doi.org/10.1016/j.nanoen.2019.104236.
10. Chen S.-W.H., Shen Ch.-Ch., Wu T. *et al*. Full-color monolithic hybrid quantum dot nanoring micro light-emitting diodes with improved efficiency using atomic layer deposition and nonradiative resonant energy transfer. *Photon. Res.* 2019. **7**, No 4. P. 416–422. https://doi.org/10.1364/PRJ.7.000416.
11. Smith R., Liu B., Bai J., Wang T. Hybrid III-nitride/organic semiconductor nanostructure with high efficiency nonradiative energy transfer for white light emitters. *Nano Lett*. 2013. **13**, No 7. P. 3042–3047. https://doi.org/10.1021/nl400597d.
12. Hedzir A.S., Sallehuddin N.N., Saidin N., Hasbullah N.F. Influence of electron irradiation on the electro-luminescence spectra of white InGaN light emitting diodes. *Ukr. J. Phys. Opt.* 2018. **19**. P. 159–164. https://doi.org/10.3116/16091833/19/3/159/2018.
13. Floriduz A., Devine J.D. Modelling of proton irradiated GaN-based high-power white light-emitting diodes. *Jpn. J. Appl. Phys*. 2018. **57**. P. 080304. https://doi.org/10.7567/JJAP.57.080304.
14. Ukolov D.S., Chirkov N.A., Mozhaev R.K., Pechenkin A.A. Radiation hardness evaluation of LEDs based on InGaN, GaN and AlInGaP hetero-structures. *IEEE 31st Int. Conf. on Microelectronics (MIEL), Nis, Serbia*. 2019. P. 197–200. https://doi.org/10.1109/MIEL.2019.8889651.
15. Gridin V.N., Ryzhikov I.V., Vinogradov V.S. A study of the effect of fast neutrons and electrons on white and blue LEDs. *Semiconductors*. 2009. **43.** P. 1690–1694. https://doi.org/10.1134/S1063782609130168.
16. Iida D., Zhuang Z., Kirilenko P. *et al*. Demonstration of low forward voltage InGaN-based red LEDs. *Appl. Phys. Exp*. 2020. **13**. P. 031001. https://doi.org/10.35848/1882-0786/ab7168.
17. Pekur D.V., Sorokin V.M., Nikolaenko Yu.E. *et al.* Determination of optical parameters in quasi-monochromatic LEDs for implementation of lighting systems with tunable correlated color temperature. *SPQEO*. 2022. **25**. P. 303–314. https://doi.org/10.15407/spqeo25.03.303.
18. Minyailo A.M., Pekur I.V., Kornaga V.I. *et al.* Optimizing the spectral composition of light from

LED phytolighting systems to improve energy efficiency. *SPQEO*. 2023. **26**. P. 463–469. https://doi.org/10.15407/spqeo26.06.463.
19. Baek S.-H., Lee H.-J., Lee S.-N. High-performance flat-type InGaN-based light-emitting diodes with local breakdown conductive channel. *Sci. Rep.* 2019. **9**. Art. No 13654. https://doi.org/10.1038/s41598-019-49727-4.

Authors' contributions

Budnyk O.P.: conceptualization, software, validation, formal analysis, investigation, visualization, writing – original draft.
Chumak M.E.: methodology, formal analysis, writing review & editing.
Stratilat D.P.: methodology, investigation, project administration.
Tartachnyk V.P.: conceptualization, formal analysis, investigation, project administration, supervision, writing – review & editing.

Authors and CV

Oksana Budnyk, PhD, researcher at the Institute of Physics, NAS of Ukraine. She received a PhD degree in Science and Technology of Materials and Nanosystems at the University of Turin, Italy. Co-author of 25 articles and 5 patents. The area of her scientific interests: microscopy and spectroscopy of biointerfaces, new materials for biosensors, optical recording and energy conversion, harvesting and storage, innovations.
https://orcid.org/0000-0001-7940-2376

Mykola Chumak, Professor, Doctor of Pedagogical Sciences, Professor of the Department of Information Technologies and Programming of the Faculty of Mathematics, Informatics and Physics, Dragomanov Ukrainian State University, Kyiv, Ukraine. Author of more than 110 publications. The area of his scientific interests: methods of solving physical problems, selected issues of theoretical physics, and ICT in education. E-mail: chumak.m.e@gmail.com, https://orcid.org/0000-0002-9956-9429

Dmytro Stratilat, Leading Engineer in the Reactor Control Group at the nuclear research reactor, Institute for Nuclear Research, NAS of Ukraine. Author of more than 10 publications. The area of his scientific interests: semiconductors with quantum wells based on InGaN nanostructures.
E-mail: reactor_104@ukr.net,
https://orcid.org/0000-0003-4682-4569

Volodymyr Tartachnyk, Doctor of Physical and Mathematical Sciences, Senior Researcher at the Department of Radiation Physics, Institute for Nuclear Research, NAS of Ukraine. Author of more than 250 publications. The area of his scientific interests: radiation and growth defects in semiconductors and kinetics of defect-impurities complexes alteration.
E-mail: tartachnyk@gmail.com,
https://orcid.org/0000-0002-6550-458X

Спектральні особливості первинних та опромінених світлодіодів InGaN з білим випромінюванням з квантовими ямами

О.П. Будник, М.Є. Чумак, Д.П. Стратілат, В.П. Тартачник

Анотація. Вимірювались спектри випромінювання білих світлодіодів (СД) InGaN/GaN, основні складові яких – лінія голубого СД з λ_{max}=443 нм та широка роздвоєна смуга вторинного випромінювання люмінофора AIT-YAG (Ce) λ = 500…650 нм. Немонотонна залежність інтенсивності свічення від температури зумовлена посиленням ефекту екранування внутрішніх полів вільними носіями, а також тепловим гасінням у результаті підвищення щільності фононного газу. В інтервалі температур 200…290 K виявлено підвищення коефіцієнта перетворення потужності випромінювання люмінофором; загальні втрати на Стоксове зміщення становлять ΔE_1 = 82%; ΔE_2 = 77% для першої і другої смуги відповідно. Сповільнення інтенсивності випромінювання при значних струмах збудження $I > 20$ мА може бути пов'язаним із балістичним перенесенням носіїв над квантовими ямами та подальшою безвипромінювальною рекомбінацією у бар'єрних шарах. Висловлюється припущення, що за існування довготривалих релаксаційних процесів у білих СД несуть відповідальність скупчення атомів In. Опромінення електронами приводить до падіння інтенсивності свічення білих СД внаслідок введення в область квантових ям глибоких безвипромінювальних рівнів радіаційних дефектів. Радіаційна стійкість люмінофора виявляється вищою від стійкості СД InGaN майже в 1,6 раза.

Ключові слова: білі СД, InGaN, AIT-YAG, гамма-опромінення, спектральні характеристики білих СД.